

Research Article

Experimental Study on the Creep Characteristics of Cemented Backfill in a Goaf under Water Pressure

JingYu Zhang,^{1,2} Huafeng Deng,² GuoYong Duan,^{2,3} LiangPeng Wan,⁴ Zuosen Luo,² and Xushu Sun ^{1,2}

¹College of Hydraulic & Environmental Engineering, China Three Gorges University, Yichang 443002, China

²Key Laboratory of Geological Hazards on Three Gorges Reservoir Area, Ministry of Education, China Three Gorges University, Yichang 443002, China

³College of Electrical Engineering & New Energy, China Three Gorges University, Yichang 443002, China

⁴China Three Gorges Projects Development CO., Ltd, Chengdu, Sichuan 610041, China

Correspondence should be addressed to Xushu Sun; sunxs@ctgu.edu.cn

Received 10 July 2020; Revised 26 October 2020; Accepted 12 November 2020; Published 27 November 2020

Academic Editor: Paweł Kłosowski

Copyright © 2020 JingYu Zhang et al. This is an open access article distributed under the Creative Commons Attribution License, which permits unrestricted use, distribution, and reproduction in any medium, provided the original work is properly cited.

As the groundwater environment changes in a goaf, the creep deformation of the backfill underwater pressure is worthy of attention. This paper takes the undercut goaf filling in the Yuzhou section of the middle route of the South-to-North Water Transfer Project as an example. Grading loading creep testing of the backfill under different water pressures was carried out using equipment developed by our research team. Based on the experimental results, the following key points were observed: (1) under the same axial stress, the creep strain and steady creep rate increase with increasing water pressure. Under the same water pressure, the creep strain and steady creep rate also increase with increasing axial stress. (2) The long-term strength of a backfill sample decreases with increasing water pressure and has a nonlinear relationship with water pressure. (3) The increase in water pressure exacerbates the damage of a backfill sample, which is manifested by the secondary crack propagation at the time of failure. Therefore, the increase in water pressure degrades the mechanical properties of the backfill to some extent. The results of this paper provide a reliable theoretical basis for the long-term stability analysis of goaf filling underwater pressure.

1. Introduction

The crossing of the water conveyance channel across a coal mine goaf is a major engineering technical problem in the Yuzhou section of the middle route of the South-to-North Water Transfer Project (as shown in Figures 1 and 2). To ensure the safety of the water conveyance channel, the goaf under the channel is filled in the early stage of the project to avoid surface deformation caused by the secondary activation of the goaf (as shown in Figure 3).

However, in the filling process, due to the complex distribution of filling material, the irregular shape of the roadway in the goaf, the consolidation settlement of the slurry, and so forth, some cavities will form in the goaf. On the other hand, with the passage of time, due to the ban on groundwater and ecological hydration in the engineering

area, the groundwater level in the goaf will rise. The groundwater will form a certain water pressure environment in the cavities of the goaf through the natural fractures in the bedrock and the fractures caused by the damage of the bedrock during the premining process (as shown in Figure 4). Therefore, the relationship between the creep mechanical properties and the long-term strength of the goaf backfill water pressure needs to be studied.

Recently, a large number of scholars have carried out a series of studies on the physical and mechanical properties of cemented backfill in goafs. The strength and deformation characteristics of the backfill are affected by factors such as temperature, acidity, alkalinity, additives, and aggregate thickness during the filling process or after filling [1–3].

Xu et al. [4] studied the fracture mechanics of cemented backfill at different temperatures by three-point bending

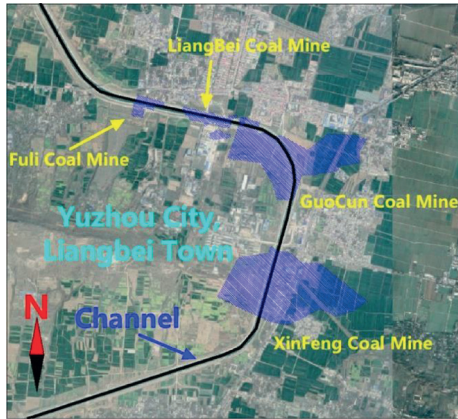


FIGURE 1: Location of channel and coal mine goaf.



FIGURE 2: South-to-North Water Transfer channel in Yuzhou city.

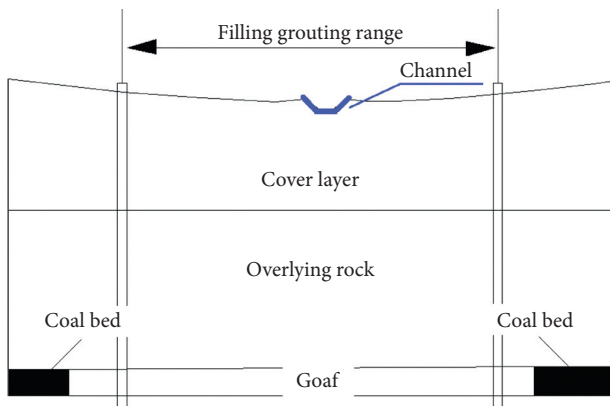


FIGURE 3: Filling range in goaf.

testing. Liu et al. [5] explored the mechanical strength of backfill in areas with lower temperatures through a series of experiments. Ercikdi et al. [6] studied the effect of temperature after dehydration on the long-term strength and creep properties of backfill. Fall and Pokharel [7] conducted temperature experiments on the mechanical properties and

microstructure of backfill and summarized its influence on the backfill integrity. Kermani et al. [8] and Hamberg et al. [9] tested the uniaxial compressive strengths of fillings from different ages and with different consolidation temperatures.

Fall and Benzaazoua [10] explored the mechanical properties of backfill in sulphate solution. Benzaazoua et al. [11] studied the effect of sulphides in tailings on the mechanical properties of backfill. Li and Fall [12] investigated the early strength of backfill influenced by sulphate. Coussy et al. [13] experimentally studied the mechanical properties of backfill under different acidity and alkalinity conditions. Liu et al. [14] explored the effect of acid corrosion on the physical and mechanical properties of full-tailings cemented backfill. The results show that the compressive strength of the cemented tailings backfill first increases and then decreases after corrosion via acidic solution. Yilmaz et al. [15, 16] studied the effect of acid hydration on the solidification and strength of backfill. Felipe-Sotelo et al. [17] explored the mechanical properties of cement fillings under alkaline conditions through experiments.

Xu et al. [18] added polypropylene fibre to the backfill to enhance its mechanical strength, thereby increasing the stability of the goaf backfill. Koupouli et al. [19] explored the shear mechanical properties between different additive fillings and retaining walls through experiments. Yilmaz et al. [20] studied the effects of three water-reducing agents on the creep and consolidation characteristics of backfill. Li et al. [21] conducted a series of experimental studies on the mechanical properties of fillings containing phosphogypsum and determined the effect of phosphogypsum on the mechanical properties of the fillings. Kesimal et al. [22] added different doses of additives to filling and performed uniaxial compressive strength tests to investigate the effects of the additives on the short-term strength and long-term strength of the filling. Olivier and Benzaazoua [23] used volcanic ash and activators to increase the mechanical strength of filling and reduce the cost of backfill.

Yin et al. [24] conducted an experimental study on the mechanical properties and creep properties of composites with different sizes of aggregates. Wang et al. [25] proposed coal gangue as an aggregate and proposed a kind of self-flow tube-filling technology for the paste. Ercikdi et al. [26] and Kesimal et al. [27] considered different sizes of aggregates in backfill and explored the influence of aggregate thickness on the mechanical properties of the backfill through experiments. Koohestani et al. [28] tested nanosilica as a filler for fine aggregates and studied the resulting viscosity and compressibility of the backfill. Fall et al. [29] studied the effects of aggregate thickness on the mechanical properties and microstructure of backfill. Kesimal et al. [30] studied the optimal particle size distribution of backfill materials. Ke et al. [31] tested the mechanical properties of different tailings backfills and explored the influence mechanism on the quality of the backfill.

Based on these research results, many studies have been carried out on the strength of cemented backfill and the deformation characteristics under stress from the four

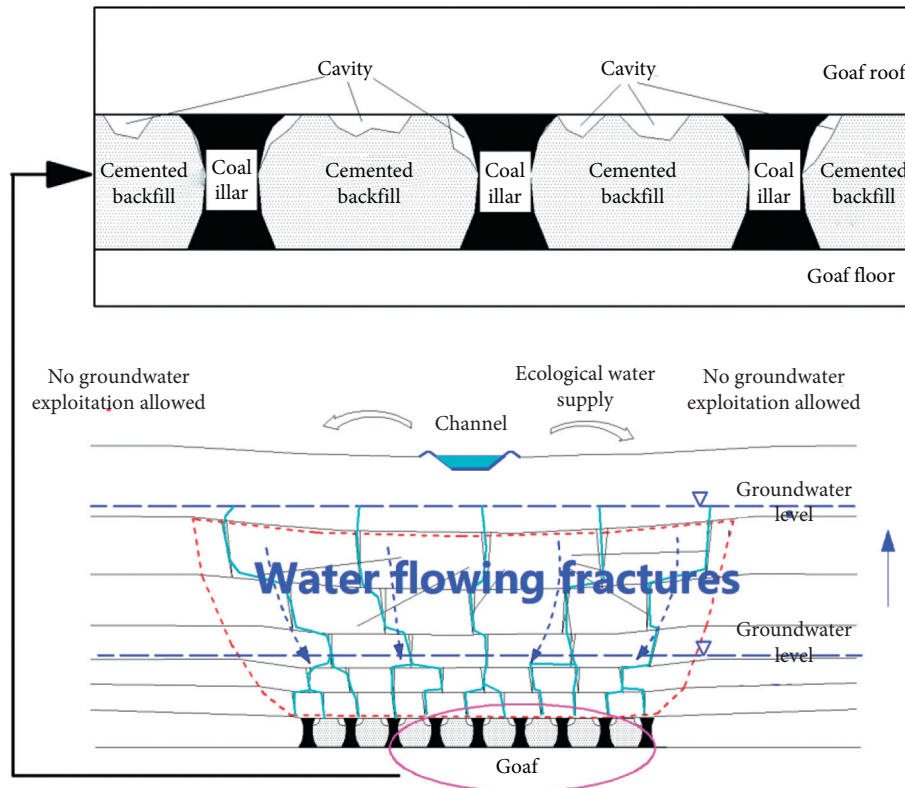


FIGURE 4: Change in the goaf groundwater environment and inadequate goaf roof-backfill connection.

aspects of temperature, chemistry (acidity and alkalinity), additives, and aggregate size (thickness). However, there are few studies on the creep properties of backfill under long-term water pressure environments. As related studies, for example, Luo et al. [32] aimed at sandstone rock slope and studied the creep characteristics of sandstone under coupled stress-water pressure. Based on the water pressure environment in goaf that may exist a long time, this paper intends to conduct an experimental study on the creep properties of goaf backfill under different water pressures.

2. Experimental Procedure

2.1. Sample Preparation. The backfill used in the test is prepared according to a mixing ratio provided in the literature [33], and the cement strength grade and water-cement ratio are shown in Table 1.

The cement, coal ash, and mould used in the test are shown in Figure 5. The backfill sample mould is 50 mm in diameter and 100 mm in height, as shown in Figure 6. The cement and coal ash were mixed according to the mixing ratio, vibrated, and poured into the mould. A selection of the 28-day-old backfill samples is shown in Figure 7.

2.2. Test Equipment. The instrument mainly used in this test is the YRQ-1000 rock immersion-air-drying cyclic load rheometer developed by the research group. The entire process is computer-controlled by the test equipment, for example, via the automatic control of the water pressure, air-

drying temperature, mixing time, shear rate, constant load, load measurement, axial deformation, water pressure, and sample temperature. The equipment can display the relationship between water pressure, temperature, normal deformation, and time in real time and the relationship between shear load and deformation after the test. The device can automatically save data, and the test data can be output in Excel format. The equipment and operation details are shown in Figure 8.

2.3. Test Equipment. First, the backfill sample is vacuumed and then immersed in water at room temperature for 48 hours to fully saturate it to simulate that the backfill has been immersed in water for a long time. The vacuuming device is shown in Figure 9.

The creep test is loaded by grading loading. Before the creep test, the instantaneous uniaxial compressive strength of the saturated backfill was measured to be approximately 8.0 MPa, as shown in Figure 10. Therefore, the first stage load of the creep test is designed to be 3.0 MPa, and each stage is increased by 1.0 MPa until damage occurs. The loading mode is shown in Figure 11, and the creep test grading loading scheme is shown in Table 2.

The depth of the coal goaf in the study area is 100~290 m. According to the relevant engineering data and the continuous rise of the groundwater level within the goaf area, the designed water pressures are 0 MPa, 0.5 MPa, 1.0 MPa, 1.5 MPa, and 2.0 MPa, respectively, simulating 0 m, 50 m, 100 m, 150 m, and 200 m water levels.

TABLE 1: Cement strength grade and water–cement ratio.

Cement strength grade	Water	42.50 MPa Cement	Coal ash
Water–cement ratio	1.00	0.15	0.85
Weight of each material	1kg	0.15 kg	0.85 kg



FIGURE 5: The cement, coal ash, and mould.

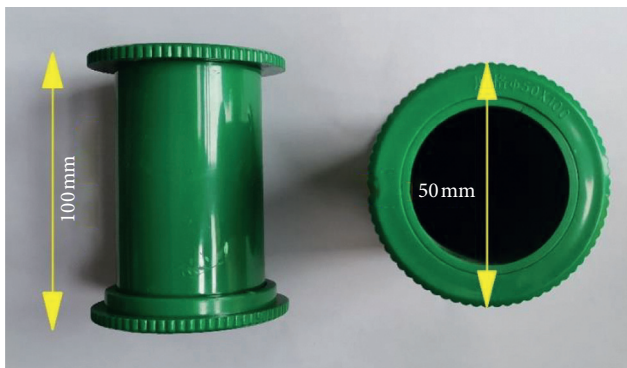


FIGURE 6: Mould size.

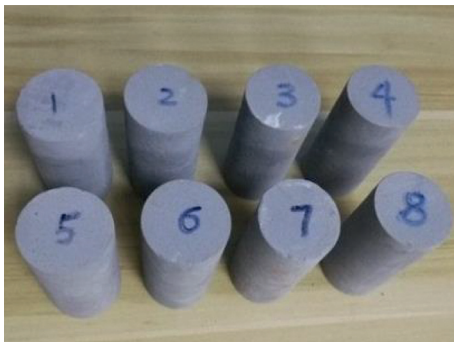


FIGURE 7: Partial backfill samples.

3. Testing Results and Analysis

The curves shown in Figure 12 are the strain–time curves of the saturated backfill sample at 0 MPa, 0.5 MPa, 1.0 MPa, 1.5 MPa, and 2.0 MPa water pressures. The creep curves of the backfill samples under both axial stress and water pressure have the following characteristics: (1) the backfill exhibits obvious transient strain and creep characteristics under various stress levels. (2) When the stress level is lower than the yield stress, the backfill sample undergoes only attenuation creep and steady-state creep. (3) When the stress level is higher than the yield stress, the backfill sample has the characteristics of not only attenuation creep and steady-state creep but also accelerated creep. (4) With the increase in water pressure, the number of creep loading stages of the backfill sample decreases, and the corresponding axial stress decreases when the backfill sample breaks.

4. Analysis of Testing Results

4.1. Analysis of Creep Deformation. The effect of axial stress and water pressure on the creep deformation characteristics of the backfill sample was studied. The cumulative total strain (including transient strain and creep strain) and the relationship between creep strain and axial stress before the failure of the backfill sample under different water pressures are plotted (as shown in Figures 13 and 14).

Figure 13 shows the following:

- (1) When the water pressure is constant, the total strain of the filling body sample increases as the axial stress increases. As the axial stress increases, the increment of cumulative total strain increases. Therefore, the greater the axial stress is, the greater the rate of change in the strain of the backfill sample.
- (2) When the axial stress is constant, the total strain of the backfill sample increases as the water pressure increases. As the water pressure increases, the increment of cumulative total strain also increases. Therefore, the greater the water pressure is, the greater the rate of change in the strain of the backfill sample.

Figure 14 shows the following:

- (1) When the water pressure is constant, the creep strain of the fill sample increases with increasing axial stress. As the axial stress increases, the increment of creep strain increases, and the creep strain increases sharply before the sample breaks. Therefore, the greater the axial stress is, the greater the rate of change in the creep strain of the backfill sample.
- (2) When the axial stress is constant, the creep strain of the fill sample increases with increasing water pressure. As the water pressure increases, the increment of creep strain also increases. Therefore, the greater the water pressure is, the greater the rate of change in the creep strain of the backfill sample.

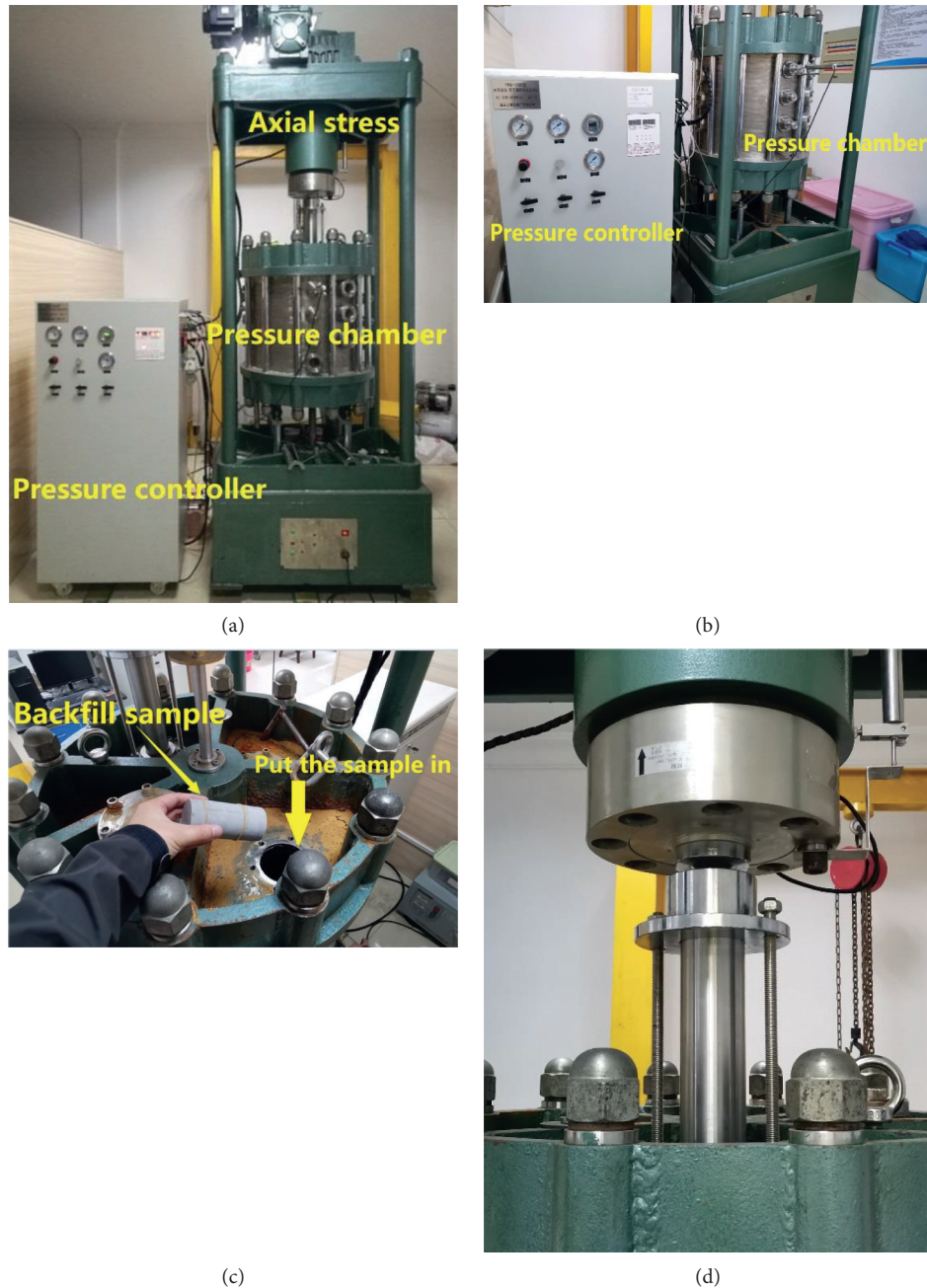


FIGURE 8: Equipment and operation details. (a) YRQ-1000 rock immersion-air-drying cyclic load rheometer. (b) YRQ-1000 rock immersion-air-drying cyclic load rheometer. (c) Putting the sample into the pressure chamber. (d) Axial loading.

In summary, under the creep test conditions, both the water pressure and axial stress will affect the creep deformation of the backfill sample. Under the same axial stress level, the greater the water pressure is, the greater the creep deformation of the backfill sample. Additionally, at the same water pressure, the greater the axial stress is, the greater the creep deformation of the backfill sample.

4.2. Analysis of Creep Rate. The slope of the creep curve for a given time is the creep rate. The slope of the creep curve can be obtained by the ratio of the creep deformation increment

to the time difference. By analyzing the data, the creep rate-time curves corresponding to different water pressures under the same axial pressure are obtained, as shown in Figure 15, in which 4.0 MPa of axial stress is taken as an example.

As shown in Figure 15, water pressure has a significant effect on the creep rate of the backfill sample. The steady creep rate of the backfill sample increases with increasing water pressure, and the time from the decay creep phase to the steady creep phase of the backfill sample is also prolonged. Thus, the water pressure has a certain softening effect on the backfill sample.

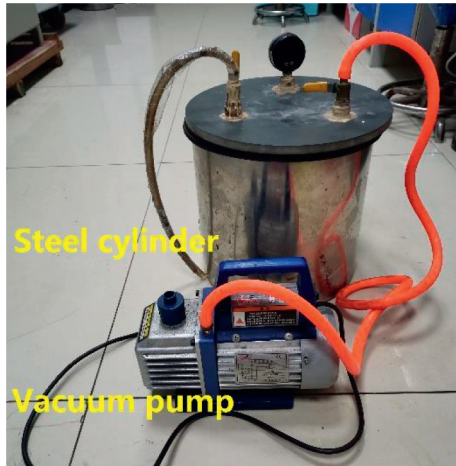


FIGURE 9: Vacuuming device.

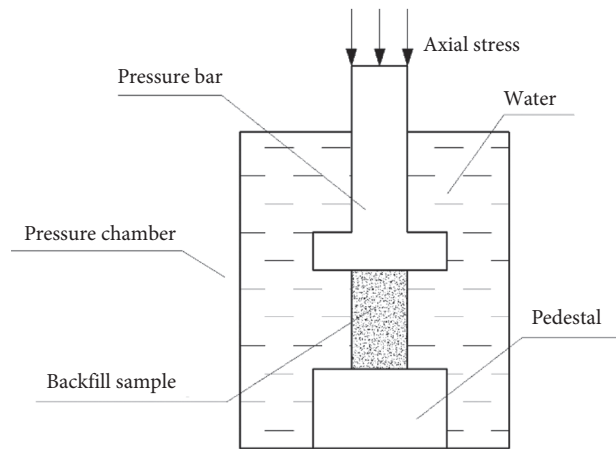


FIGURE 11: Creep loading method.

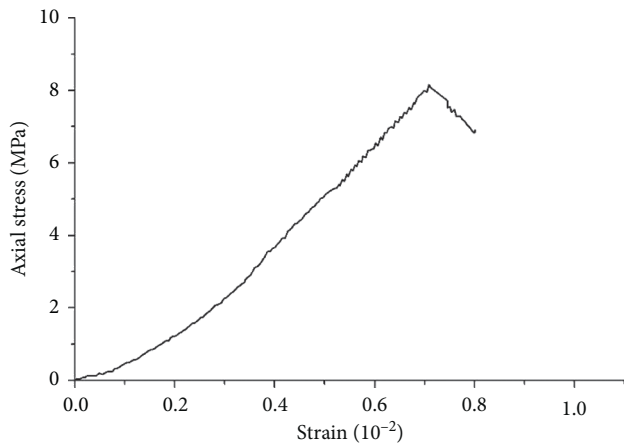


FIGURE 10: Stress-strain curve of uniaxial compression test of backfill.

By analyzing the test data, the creep rate-time curves corresponding to different axial pressures at the same water pressure are obtained, as shown in Figure 16, taking 1.0 MPa of water pressure as an example.

As shown in Figure 16, axial stress also has a significant effect on the creep rate of the samples. The creep rate of a backfill sample also increases with axial stress. When the axial stress reaches the yield stress of the backfill sample, the creep rate of the backfill sample increases considerably. After a short period of steady creep, the backfill sample enters the accelerated creep stage until the sample is destroyed.

4.3. Analysis of Long-Term Strength. A large number of laboratory tests and engineering examples show that rock and rock-like materials will also be damaged by long-term loads with magnitudes below the peak strength. The strength decreases with increasing load action time. When the time is extended, the corresponding load becomes the long-term strength of the material when the material is destroyed. In this paper, the isochronous curve method is used to

TABLE 2: Creep loading scheme.

Water pressure (MPa)	Axial stress (MPa)				
	1 st level	2 nd level	3 rd level	4 th level	5 th level
0	3.0	4.0	5.0	6.0	7.0
0.5	3.0	4.0	5.0	6.0	—
1.0	3.0	4.0	5.0	6.0	—
1.5	3.0	4.0	5.0	—	—
2.0	3.0	4.0	5.0	—	—

determine the long-term strengths of the backfill samples under different water pressures [34].

Table 3 and Figure 17 show the following:

- (1) With the increase in water pressure, the long-term strength of a backfill sample shows a decreasing trend, indicating that the increase in water pressure has a significant deteriorating effect on the mechanical properties of the backfill sample.
- (2) There is a nonlinear relationship between the long-term strength of a backfill sample and the water pressure. This relationship can be accurately fitted by a quadratic polynomial function:

$$\sigma = ap^2 + bp + c, \quad (1)$$

where σ is long-term strength; a , b , and c are coefficients; and p is water pressure.

The fitting formula can be written as

$$\sigma = 0.34p^2 - 1.71p + 6.76. \quad (2)$$

As the water pressure increases from 1.5 MPa to 2.0 MPa, the decrease in long-term strength decreases.

- (3) The long-term strengths of the backfill samples at 0 MPa, 0.5 MPa, 1.0 MPa, 1.5 MPa, and 2.0 MPa water pressures are 6.71 MPa, 6.12 MPa, 5.31 MPa,

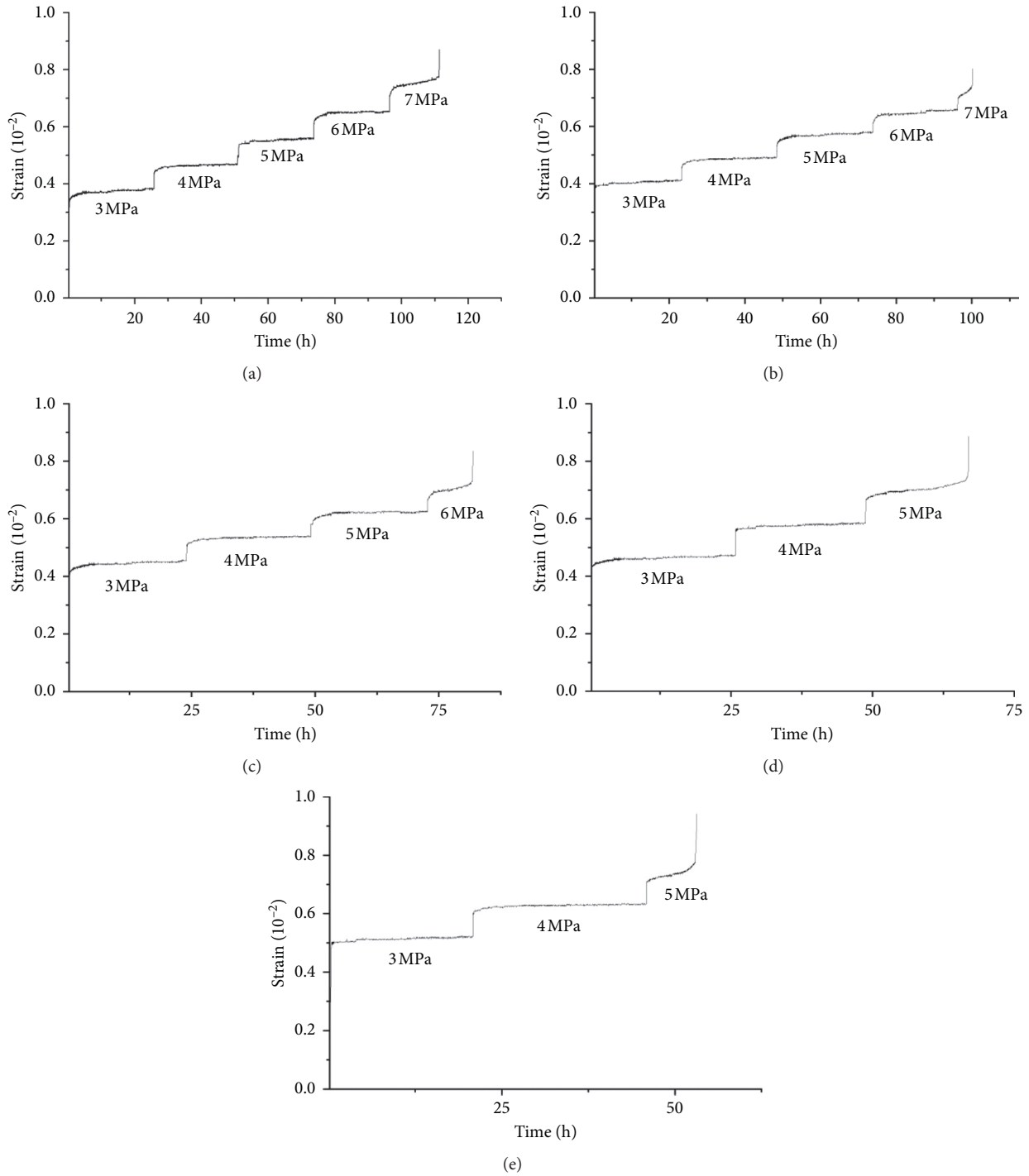


FIGURE 12: Creep test strain–time curve of backfill under different water pressures. (a) 0 MPa water pressure. (b) 0.5 MPa water pressure. (c) 1.0 MPa water pressure. (d) 1.5 MPa water pressure. (e) 2.0 MPa water pressure.

4.93 MPa, and 4.72 MPa, respectively. The degradation ratios are 0%, 8.8%, 20.9%, 26.5%, and 29.6%, respectively. As the water pressure increases, the degree of deterioration of the filling body increases continuously, but the rate of deterioration gradually decreases. It can be inferred that when the water pressure increases to a certain magnitude, the long-

term strength of the backfill sample will approach a certain magnitude.

4.4. Analysis of Destructive Features. The failure mode diagrams and crack drawings of the backfill samples under different water pressures are shown in Figure 18.

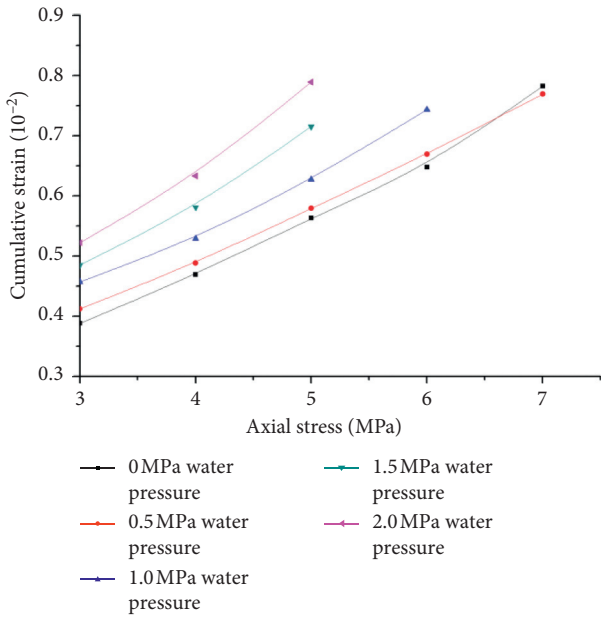


FIGURE 13: Cumulative strain-axial stress curve under different water pressures.

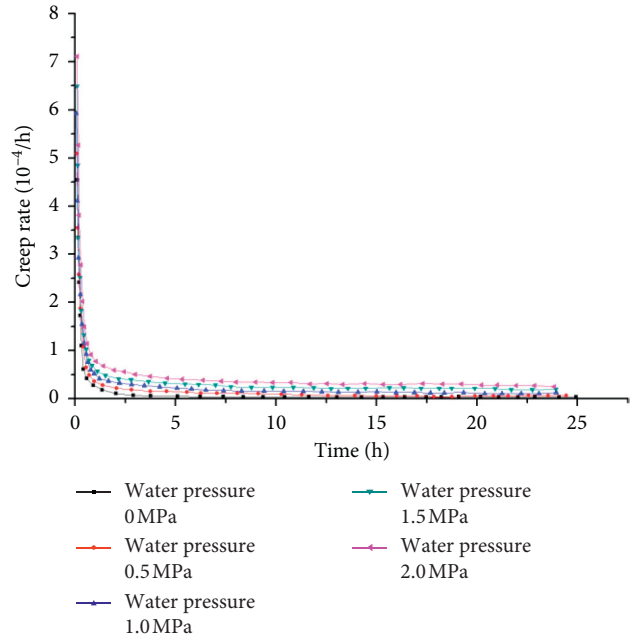


FIGURE 15: The creep rate under different water pressures at 4.0 MPa axial pressure.

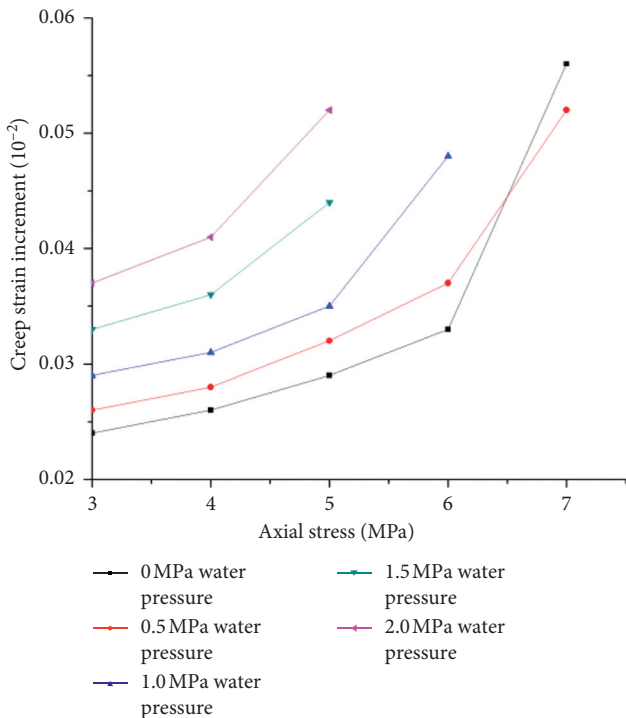


FIGURE 14: Creep increment-axial stress curve under different water pressures.

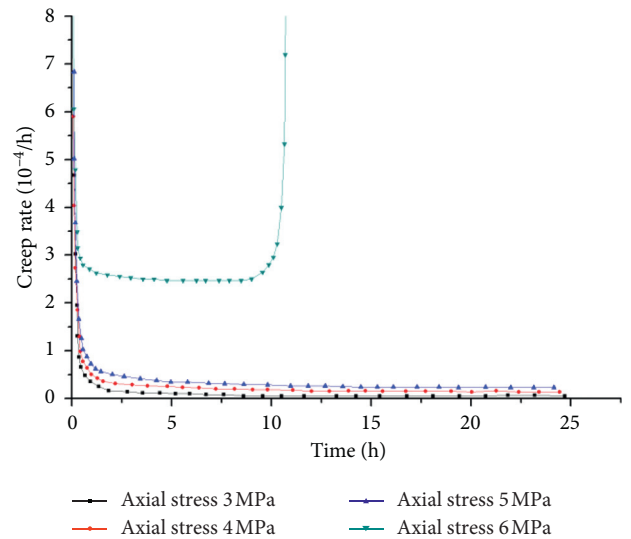


FIGURE 16: The creep rate under different axial pressures and 1.0 MPa water pressure.

Figure 18 shows the similarities and differences among the failure modes of the backfill samples under different water pressures:

- (1) From the overall failure mode of the backfill sample, the creep failure characteristics of the backfill sample

under different water pressures show obvious shear failure characteristics. The cracks basically initiate at one end face of the backfill sample and propagate to the other end face. When the backfill sample is broken, one or two interconnected shear faces are observed.

- (2) When the water pressure is 0 MPa, the number of cracks observed after the sample is destroyed is small. When the water pressure is 0.5 MPa, the number of cracks observed after the sample is damaged is higher, and some main cracks exhibit obvious bifurcation. When the water pressure is 1.0 MPa, the

TABLE 3: Long-term strengths under different water pressures.

Water pressure (MPa)	Long-term strength (MPa)	Degradation ratio (%)
0	6.71	0
0.5	6.12	8.8
1.0	5.31	20.9
1.5	4.93	26.5
2.0	4.72	29.6

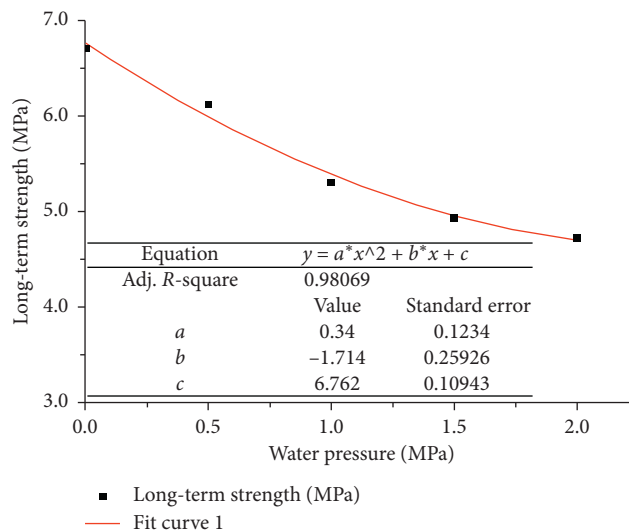


FIGURE 17: Relationship between long-term strength and water pressure.

main crack bifurcation phenomenon becomes increasingly obvious. When the water pressure is 1.5 MPa, the main crack not only branches but also generates secondary cracks. When the water pressure is 2.0 MPa, one main crack generates more secondary cracks than the main crack under a water pressure of 1.5 MPa generates.

In general, under the action of low water pressure, the shape of the main crack is relatively simple when the backfill sample is broken, and fewer secondary cracks form. However, under the action of higher water pressure, the main crack is accompanied by a certain number of secondary cracks when the fill sample is broken. This difference is mainly due to the increase in water pressure, which causes the microcracks in the backfill sample to expand inward. At the same time, under the axial load, these microcracks are subjected to compression and shearing, and stress concentrations are generated at the crack tips.

5. Discussion of the Effect of Water Pressure and Axial Stress on a Sample

A backfill sample is affected by water pressure and axial pressure, under which the long-term strength of the sample is continuously degraded.

There are two main reasons for this change in strength. (1) The pore water pressure in a saturated backfill sample will increase from the surface to the interior. During this process, the pore water pressure inside the sample increases as the external water pressure increases. The tensile stress at the tip of a microcrack is sharply increased, causing the microcrack to expand inward (as shown in Figure 19) and causing the mechanical properties of the fill sample to deteriorate to different degrees. (2) The increase in axial stress also causes a stress concentration (tensile stress or shear stress or compressive stress) to form at the tip of the microcrack, which accelerates the expansion of microcracks in the fill sample (as shown in Figure 20). The new cracks continue to expand under the action of the water pressure and axial stress, which further deteriorates the mechanical properties of the backfill sample. Therefore, during the test, the creep deformation of fill samples is more obvious under the action of higher water pressures and higher axial stresses.

In addition, when the water pressure is constant, as the axial pressure increases, the rate of steady-state creep increases but the time of steady-state creep stage becomes shorter, while the rate of decay creep increases but the time of decay creep stage becomes longer. When the axial pressure is constant, as the water pressure increases, the rate of steady-state creep increases and the time of steady-state creep stage becomes shorter, while the rate of decay creep increases but

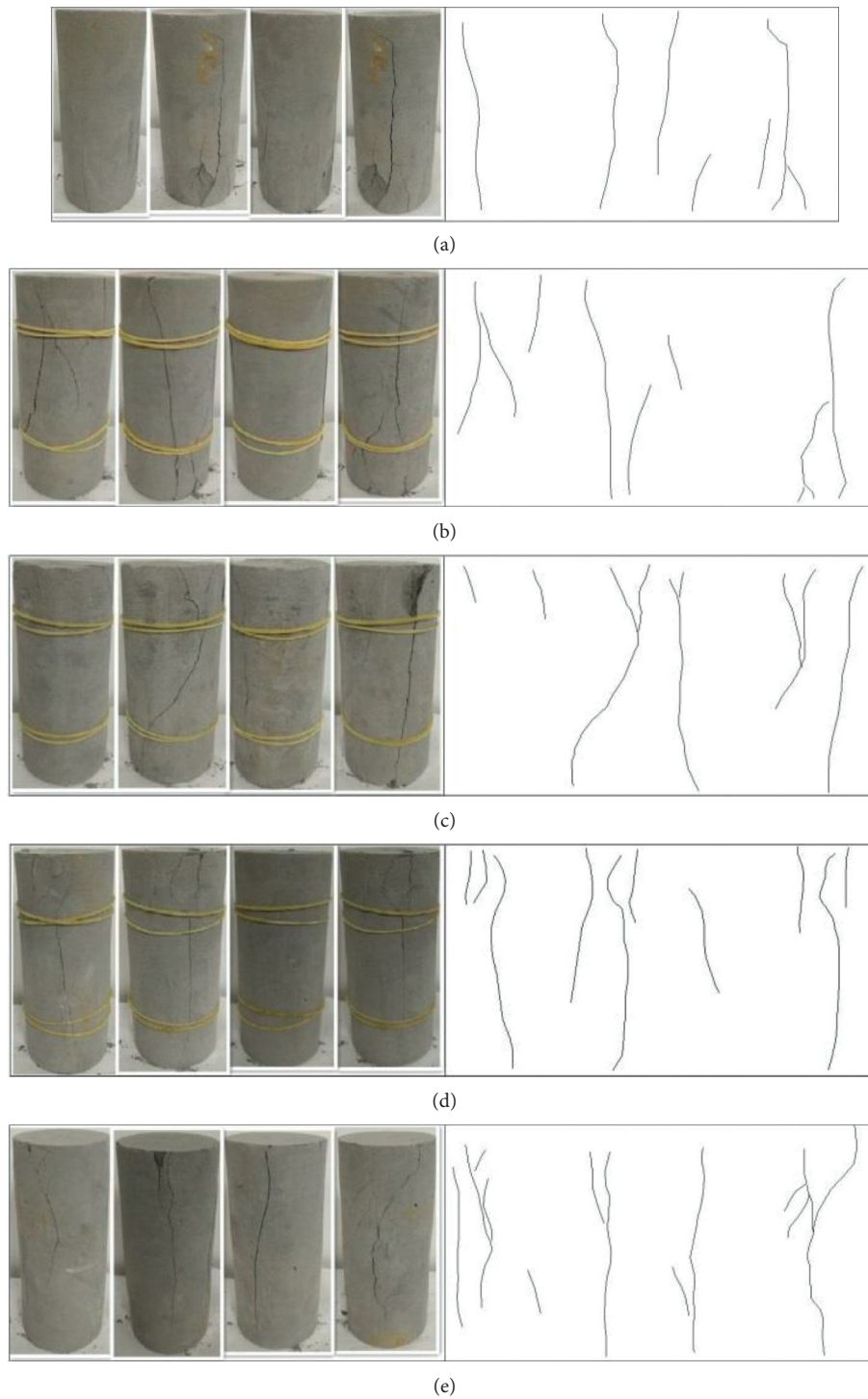


FIGURE 18: Failure mode of backfill samples under different water pressures. (a) 0 MPa water pressure. (b) 0.5 MPa water pressure. (c) 1.0 MPa water pressure. (d) 1.5 MPa water pressure. (e) 2.0 MPa water pressure.

the time of decay creep stage becomes longer. This shows that the sample is damaged in the process of increasing water pressure and axial pressure, and the number of microcracks

inside the sample is increasing, which leads to the increase of the rate in the creep stage and finally shows the phenomenon that the long-term strength of the sample decreases.

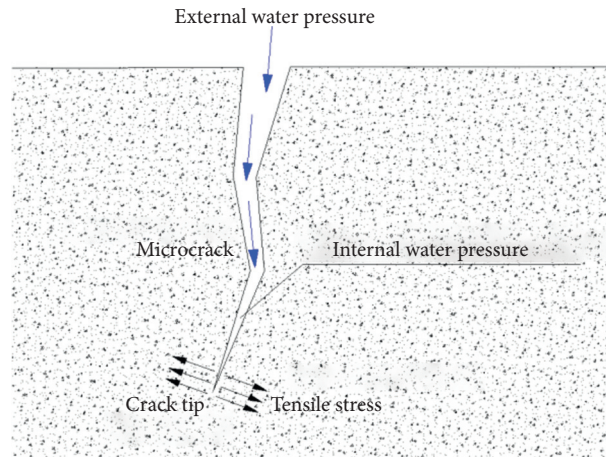


FIGURE 19: Microcrack propagation as water pressure increases.

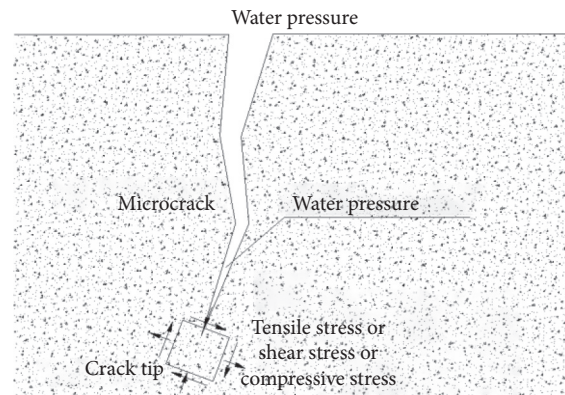


FIGURE 20: Microcrack propagation as axial stress increases.

6. Conclusions

In this paper, creep testing of goaf backfill under the combined action of water pressure and stress is carried out, and the following conclusions are obtained:

- (1) Under the same axial stress, the increase in water pressure increases the creep strain and initial creep rate of a backfill sample, prolongs the duration of decay creep to steady creep, and increases the steady creep rate. Similarly, under the same water pressure, the increase in axial stress also increases the creep strain and initial creep rate of a backfill sample, prolongs the duration of decay creep to steady creep, and increases the steady creep rate.
- (2) As the water pressure increases, the long-term strength of a backfill sample gradually decreases, and as the water pressure increases to 1.5 MPa, the long-term strength reduction decreases. This result indicates that the increase in water pressure degrades the mechanical properties of the backfill sample, causing the backfill sample to enter the yield stage earlier. However, the influence of the water pressure on the long-term strength of a fill sample is limited. The long-term strength of a fill sample will gradually

approach a certain value with increasing water pressure.

- (3) The increase in water pressure exacerbates the development of cracks during failure of the fill sample. As the water pressure increases, the damage caused by the water pressure inside the backfill sample also accumulates, causing the internal microcracks to expand. Under the action of axial stress, the secondary cracks increase significantly during the failure of the backfill.
- (4) Most coal mines contain sulfur, phosphorus, and other elements. Therefore, in addition to water pressure and axial pressure of goaf roof, the pH value of water should also be considered. Long-term immersion of backfill body in acidic water solution will also accelerate the deterioration of its long-term strength. In the later research, the creep characteristics of backfill under the combined action of different pH values and axial pressure of water pressure will be considered.

Data Availability

The data used to support the findings of this study may be released upon application to the China Three Gorges

University Review Board, which can be done by contacting Jingyu Zhang (zjy7268@sina.com).

Conflicts of Interest

The authors wish to confirm that there are no known conflicts of interest associated with this publication and there has been no significant financial support for this work that could have influenced its outcome. Accordingly, the alteration of confining pressure is of most significant on the variation of the tensile stress while the joint angle contributes the minimal impact.

Acknowledgments

This research was supported by the National Nature Science Foundation of China (51679127), Key Projects of Science and Technology Research Plan of Educational Commission of Hubei Province (D20181202), and Construction and Management of Hydropower Project Open Fund of Hubei Key Laboratory (2019KSD10).

References

- [1] Y. Wang, A. X. Wu, H. J. Wang et al., "Damage constitutive model of cemented tailing paste under initial temperature effect," *Chinese Journal of Engineering*, vol. 39, no. 1, pp. 31–38, 2017.
- [2] Y. Wang, M. Fall, and A. Wu, "Initial temperature-dependence of strength development and self-desiccation in cemented paste backfill that contains sodium silicate," *Cement and Concrete Composites*, vol. 67, pp. 101–110, 2016.
- [3] M. Fall, J. C. Célestin, M. Pokharel et al., "A contribution to understanding the effects of curing temperature on the mechanical properties of mine cemented tailings backfill," *Engineering Geology*, vol. 114, pp. 397–413, 2010.
- [4] W. Xu, P. Cao, and S. Cheng, "Study on fracture characteristics and crack propagation mode of cemented backfill in deep mine," *Journal of Central South University (Science and Technology)*, vol. 49, no. 10, pp. 2508–2518, 2018.
- [5] C. Liu, B. Han, W. Sun et al., "Experimental study of strength of backfillings of cemented rock debris and its application under low temperature condition," *Chinese Journal of Rock Mechanics and Engineering*, vol. 34, no. 1, pp. 139–147, 2015.
- [6] B. Ercikdi, H. Baki, and M. İzki, "Effect of desliming of sulphide-rich mill tailings on the long-term strength of cemented paste backfill," *Journal of Environmental Management*, vol. 115, pp. 5–13, 2013.
- [7] M. Fall and M. Pokharel, "Coupled effects of sulphate and temperature on the strength development of cemented tailings backfills: Portland cement-paste backfill," *Cement & Concrete Composites*, vol. 32, pp. 819–828, 2010.
- [8] M. Kermani, F. P. Hassani, E. Aflaki et al., "Evaluation of the effect of sodium silicate addition to mine backfill, Gelfill-part 2: effects of mixing time and curing temperature," *Journal of Rock Mechanics and Geotechnical Engineering*, vol. 7, pp. 668–673, 2015.
- [9] R. Hamberg, C. Maurice, and L. Alakangas, "The use of low binder proportions in cemented paste backfill - effects on as-leaching," *Minerals Engineering*, vol. 78, pp. 74–82, 2015.
- [10] M. Fall and M. Benzaazoua, "Modeling the effect of sulphate on strength development of paste backfill and binder mixture optimization," *Cement and Concrete Research*, vol. 35, pp. 301–314, 2005.
- [11] M. Benzaazoua, B. Bruno, I. Demers et al., "Integrated mine tailings management by combining environmental desulphurization and cemented paste backfill: application to mine Doyon, Quebec, Canada," *Minerals Engineering*, vol. 21, pp. 330–340, 2008.
- [12] W. Li and M. Fall, "Sulphate effect on the early age strength and self-desiccation of cemented paste backfill," *Construction and Building Materials*, vol. 106, pp. 296–304, 2016.
- [13] S. Coussy, M. Benzaazoua, D. Blanc et al., "Arsenic stability in arsenopyrite-rich cemented paste backfills: a leaching test-based assessment," *Journal of Hazardous Materials*, vol. 185, pp. 1467–1476, 2011.
- [14] W. Liu, Y. Rao, W. Xu et al., "Effect of acidic corrosion on physical and mechanical properties of full tailing cemented backfill," *Mining Research and Development*, vol. 38, no. 3, pp. 91–93, 2018.
- [15] E. Yilmaz, M. Benzaazoua, T. Belem et al., "Effect of curing under pressure on compressive strength development of cemented paste backfill," *Minerals Engineering*, vol. 22, pp. 772–785, 2009.
- [16] E. Yilmaz, T. Belem, and M. Benzaazoua, "Effects of curing and stress conditions on hydromechanical, geotechnical and geochemical properties of cemented paste backfill," *Engineering Geology*, vol. 168, pp. 23–37, 2014.
- [17] M. Felipe-Sotelo, J. Hinchliff, L. P. Field et al., "The solubility of nickel and its migration through the cementitious backfill of a geological disposal facility for nuclear waste," *Journal of Hazardous Materials*, vol. 314, pp. 211–219, 2016.
- [18] X. W. Yi, G. W. Ma, and A. Fourie, "Compressive behaviour of fibre-reinforced cemented paste backfill," *Geotextiles and Geomembranes*, vol. 43, pp. 207–215, 2015.
- [19] N. J. F. Milodowski, T. Belem, P. Rivard et al., "Direct shear tests on cemented paste backfill-rock wall and cemented paste backfill-backfill interfaces," *Journal of Rock Mechanics and Geotechnical Engineering*, vol. 8, pp. 472–479, 2016.
- [20] E. Yilmaz, T. Belem, B. Bussi ere, M. Mbonimpa, and M. Benzaazoua, "Curing time effect on consolidation behaviour of cemented paste backfill containing different cement types and contents," *Construction and Building Materials*, vol. 75, pp. 99–111, 2015.
- [21] X. Mbonimpa, J. Du, L. Gao et al., "Immobilization of phosphogypsum for cemented paste backfill and its environmental effect," *Journal of Cleaner Production*, vol. 156, pp. 137–146, 2017.
- [22] A. He, E. Yilmaz, B. Ercikdi et al., "Effect of properties of tailings and binder on the short-and long-term strength and stability of cemented paste backfill," *Materials Letters*, vol. 59, pp. 3703–3709, 2005.
- [23] P. Olivier and M. Benzaazoua, "Alternative by-product based binders for cemented mine backfill: recipes optimisation using," *Minerals Engineering*, vol. 29, pp. 28–38, 2012.
- [24] S. Yin, A. Wu, K. Hu, Y. Wang, and Y. Zhang, "The effect of solid components on the rheological and mechanical properties of cemented paste backfill," *Minerals Engineering*, vol. 35, pp. 61–66, 2012.
- [25] X. M. Wang, B. Zhao, C. S. Zhang et al., "Paste-like self-flowing transportation backfilling technology based on coal gangue," *Mining Science and Technology*, vol. 19, pp. 0137–0143, 2009.
- [26] B. Ercikdi, G. K ulekci, and T. Yilmaz, "Utilization of granulated marble wastes and waste bricks as mineral admixture in

- cemented paste backfill of sulphide-rich tailings,” *Construction and Building Materials*, vol. 93, pp. 573–583, 2015.
- [27] A. Kesimal, E. Yilmaz, and B. Ercikdi, “Evaluation of paste backfill mixtures consisting of sulphide-rich mill tailings and varying cement contents,” *Cement and Concrete Research*, vol. 34, pp. 1817–1822, 2004.
- [28] B. Koohestani, T. Belem, A. Koubaa, and B. Bruno, “Experimental investigation into the compressive strength development of cemented paste backfill containing nano-silica,” *Cement and Concrete Composites*, vol. 72, no. 72, pp. 180–189, 2016.
- [29] M. Bussi ere, M. Benzaazoua, and S. Ouellet, “Experimental characterization of the influence of tailings fineness and density on the quality of cemented paste backfill,” *Minerals Engineering*, vol. 18, pp. 41–44, 2005.
- [30] A. Kesimal, B. Ercikdi, and E. Yilmaz, “The effect of desliming by sedimentation on paste backfill performance,” *Minerals Engineering*, vol. 16, pp. 1009–1011, 2003.
- [31] X. Ke, H. Hou, M. Zhou, Y. Wang, and X. Zhou, “Effect of particle gradation on properties of fresh and hardened cemented paste backfill,” *Construction and Building Materials*, vol. 96, pp. 378–382, 2015.
- [32] Z. Wang, J. Li, L. Wang et al., “Study on the creep characteristics of sandstone under coupled stress-water pressure,” *Periodica Polytechnica Civil Engineering*, vol. 63, no. 4, pp. 1038–1051, 2019.
- [33] F. Wei, “Quality control of grouting slurry in coal mined-out area in Yuzhou city of middle route project of South to North Water diversion,” *Yangtze River*, vol. 45, no. 10, pp. 87–93, 2014.
- [34] J. Sun, “Rock rheological mechanics and its advance in engineering applications,” *Chinese Journal of Rock Mechanics and Engineering*, vol. 26, no. 6, pp. 1081–1106, 2007.